Am J Transl Res 2021;13(4):2350-2364
www.ajtr.org /ISSN:1943-8141/AJTR0118135

Original Article

Elevating miR-378 strengthens the isoflurane-mediated effects on myocardial ischemia-reperfusion injury in mice via suppression of MAPK1

Rui Zhou[1], Yingping Jia[1], Yuan Wang[1], Zhengchen Li[1], Jinlian Qi[1], Yanmei Yang[2]

[1]Anesthesia and Perioperative Medicine, The Affiliated Children's Hospital of Zhengzhou University, Henan Children's Hospital, Zhengzhou Children's Hospital, Zhengzhou 450018, Henan, China; [2]Anesthesiology Department, Kaifeng District of No.988 Hospital, PLA's Logistic Support Department, Kaifeng 475003, Henan, China

Received July 14, 2020; Accepted February 5, 2021; Epub April 15, 2021; Published April 30, 2021

Abstract: Objective: Myocardial ischemia reperfusion (MI/RI) stresses the pathological process of progressive aggravation of tissue damage in ischemic myocardium. Isoflurane (ISO) is cardioprotective in MI/RI. Thus, this work aimed to identify the mechanism of isoflurane (ISO) post-treatment in MI/RI by regulating microRNA-378 (miR-378) and mitogen-activated protein kinase 1 (MAPK1). Methods: A MI/RI model was established by ligating the left anterior descending coronary artery in mice. The modeled mice were injected with ISO or miR-378 or MAPK1 to define their roles in hemodynamics, myocardial injury, cell apoptosis and inflammatory infiltration of mice. CD45, miR-378 and MAPK1 levels were detected. Dual luciferase reporter gene assay was utilized for detection of the targeting connection of miR-378 and MAPK1. Results: Reduced miR-378 and elevated MAPK1 existed in MI/RI. ISO elevated miR-378 to target MAPK1. ISO improved hemodynamics and myocardial injury, reduced apoptosis rate and inflammatory infiltration in MI/RI mice. Up-regulated miR-378 further enhanced the protective effect of ISO on MI/RI mice. Depleting MAPK1 reversed the effects of suppressed miR-378 on MI/RI. Conclusion: This study highlights that elevating miR-378 strengthens the isoflurane-mediated effects on MI/RI in mice via suppressing MAPK1, which provides a potential treatment for MI/RI.

Keywords: Myocardial ischemia reperfusion injury, isoflurane post-treatment, microRNA-378, mitogen-activated protein kinase 1, apoptosis, myocardial infarction, inflammatory infiltration, hemodynamics

Introduction

Myocardial ischemia reperfusion injury (MI/RI) refers to the progress that persistent reperfusion after ischemia frequently leads to secondary damage to the myocardium [1]. MI/RI is a main cause for damage in cardiac tissues with high rates of mortality and disability [2]. Moreover, MI/RI also results in serious arrhythmias with great lethality [3]. Ultrasound is a prevailing approach to protect against MI/RI [4]. MI/RI can stimulate the cardiomyocyte apoptosis and necrosis or even cardiac arrest, thereby affecting the treatment outcome of heart diseases [5]. Therefore, it is of great importance to clarify the exact mechanism of the occurrence and development of MI/RI and to find early diagnostic markers and therapeutic targets for MI/RI.

Isoflurane (ISO) is a commonly-functioned inhalational anesthetic medicine [6]. A therapy with ISO has been reported to ameliorate MI/RI in rodents and patients [7]. In addition, ISO pretreatment in the delayed period has protective influences on a rabbit model of I/RI [8]. MicroRNAs (miRNAs) take part in the modulation of target genes at the post-transcriptional level [9]. MiR-378 is regarded as a vital regulator and a therapeutic target in intestinal I/R injury [10]. Meanwhile, miR-378 relieves ischemic injury, offering a possible therapeutic target for ischemic stroke in cerebral ischemic injury [11]. The mitogen-activated protein ki-

nase (MAPK) is the protein kinase that includes serine-threonine kinases and greatly conserves in the progression of biological evolution [12]. Repressing the MAPK pathway is implicated with AAV9-TLR4 siRNA's positive influence on MI/RI, which can be utilized as a possible therapeutic way for MI/RI [13]. Also, suppressing the MAPK signaling pathway is associated with butorphanol regulation of the recovery of the myocardial injury in the rats after MI/RI [14]. Furthermore, an article has demonstrated that MAPK1 is implicated with testicular I/R injury [15]. Hence, the goal of the study was to clarify the mechanism of ISO post-treatment in mice with MI/RI through miR-378/MAPK1 axis.

Materials and methods

Ethics statement

The protocol was permitted by the Institutional Animal Care and Use Committee of No.988 Kaifeng hospital, joint logistic support force of the PLA. Efforts were made to avoid all unnecessary distress to the animals in compliance with the recommendations in the Guide for the Care and Use of Laboratory Animals of the National Institutes of Health.

Experimental animals

Female C57BL/6 mice aged 8 weeks, weighed 18-20 g, were purchased from the Laboratory Animal Center Zhengzhou University (Henan, China) and kept in specific pathogen-free grade animal cages (n = 5/cage) in the Animal Experimental Center of No.988 Kaifeng hospital, joint logistic support force of the PLA. The environmental conditions were set with 12 h: 12 h light-darkness living mode and 50%-60% relative humidity at 20-22°C. The mice were fed with conventional pellet feed and free to drink and eat.

Establishment of MI/RI model

C57BL/6 mice were fixed in a supine position, anesthetized via intraperitoneal injection of pentobarbital sodium (30 mg/kg). II lead electrocardiogram was connected with the mice which were cleaned and disinfected with 75% absolute ethyl alcohol in neck and chest. Through a central incision about 1 cm below the neck, the jugular anterior fascicles were implemented blunt dissection along the midline to expose the trachea. The mice were intubated in trachea from the mouth of mice, the cannula was fixed and the ventilator was quickly connected to assist breathing. A longitudinal incision was made on the left side of the sternum and the fourth costicartilage was cut at about 0.5 cm of left margin of the sternum. The heart was exposed, and the ligation was performed with a non-invasive needle at about 1/3 of the left anterior descending branch of the coronary artery with a depth of about 1.5 mm. Successful modeling was confirmed by darker myocardium at the distal end of the ligation and raised ST-segment of the electrocardiogram (15 mice of failed modeling).

Treatment of animals

The mice were divided into 8 groups (n = 15). Sham-operated mice were treated with threading without ligation. The mice for modeling were treated with ischemia for 30 min and reperfusion for 2 h. Five days before modeling, miR-378 or anti-miR-378 was injected into the caudal vein for 3 d, while si-MAPK1 (2×10^7 pfu/mL) was injected into the myocardium after 3-d injection of anti-miR-378 [16]. ISO post-treatment (1.0 MAC) was performed for 30 min after modeling [17]. After 30 min of the last administration, mice were euthanized by neck dislocation.

Hemodynamic indices test

Six mice were randomly selected from each group, and the right common carotid artery was intubated to the left ventricle. The pressure sensor was connected to the biological signal acquisition and analysis system to record left ventricular systolic pressure (LVSP), left ventricular end diastolic pressure (LVEDP), maximal rate of the increase/decrease of left ventricular pressure ($+dp/dt_{max}$/$-dp/dt_{max}$).

Specimen collection and treatment

The blood and heart tissues were collected, and the myocardial tissues of mice (n = 5) were fixed in 4% paraformaldehyde, dehydrated with conventional alcohol, cleared with xylene, embedded in paraffin and cut into slices of 5 μm for hematoxylin-eosin (HE) staining, CD45 detection and apoptosis detection. After rinsed with cold phosphate buffered saline (PBS), the myocardial tissues from another 10 mice were

immediately frozen in liquid nitrogen and stored at -80°C. The blood was allowed to stand for 2 h, and centrifuged at 3000 rpm for 20 min, and then the upper serum was absorbed and stored at -20°C.

Inflammatory factor detection

The contents of tumor necrosis factor-α (TNF-α), interleukin (IL)-1β, and IL-6 were detected in serum with the enzyme-linked immunosorbent assay (ELISA) kit (Labsystems, Helsinki, Finland).

Detection of myocardial enzyme and oxidative stress-related factors

The serum of mice (n = 5) was harvested for detection of myocardial enzymes and oxidation stress-related indices. Myocardial enzymes and oxidative stress-related factors were detected via automatic biochemical analyzer (Beckman Coulter Life Sciences, Brea, CA California, USA) with the detection kit (NanJing JianCheng Bioengineering Institute, Nanjing, China).

Myocardial enzymes: aspartic amino-transferase (AST), creatine kinase (CK), creatine kinase isoenzyme (CK-MB) and lactate dehydrogenase (LDH). Oxidative stress-related factors: superoxide dismutase (SOD), malondialdehyde (MDA), glutathione peroxidase (GSH-Px), catalase (CAT) and nitric oxide (NO).

HE staining

The paraffin sections were dried at 60°C, dehydrated with conventional gradient alcohol, and cleared with xylene. Then the tissue sections were stained with hematoxylin solution, differentiated with 1% hydrochloric acid alcohol, and treated with 1% ammonium hydroxide. The tissue sections were counter-stained with 1% eosin solution, followed by conventional dehydration (75%, 90%, 95%, anhydrous ethanol), xylene clearance and sealed. The sections were observed under a microscope and photographed.

Terminal deoxynucleotidyl transferase-mediated deoxyuridine triphosphate-biotin nick end-labeling (TUNEL) staining

Paraffin sections were routinely dewaxed and hydrated, and rinsed with 0.1 M PBS (pH 7.4) for 3 times, 5 min once. Then the sections were detached with 20 μg/mL protease K for 20 min, and incubated with 0.1% Triton X-100 for 4 min and 3% H_2O_2. The sections were incubated with freshly prepared TUNEL reaction solution, dripped with 50 mL C tube liquid, and developed via diaminobenzidine (DAB). The sections were counterstained with hematoxylin solution, soaked in alcohol, treated with xylene, and sealed with neutral gum. TUNEL-positive cardiomyocytes were those with brownish yellow nucleus observed under the light microscope. The apoptosis rate = the number of positive cells/the number of total cells × 100%. TUNEL kit was purchased from Roche Diagnostics (Indianapolis, IN, USA).

Immunohistochemistry

Paraffin sections were routinely dewaxed, immersed in ethylene diamine tetraacetic acid antigen retrieval solution for 20 min and incubated with endogenous peroxidase blocker for 20 min. The tissues were treated with primary antibody CD45 (1:50, Invitrogen, Carlsbad, California, USA), enhanced chemiluminescence for 30 min and with the second antibody for 90 min. Developed via DAB, the sections were counterstained with hematoxylin for 35 s, differentiated, dehydrated, sealed and observed under a microscope.

Reverse transcription quantitative polymerase chain reaction (RT-qPCR)

The total RNA in myocardial tissues was extracted via using miRNeasy Mini kit (Qiagen, Hilden, Germany). The RNA samples were reversely transcribed by TaqMan® MicroRNA reverse transcription kit (Applied Biosystems, Foster City, CA, USA). PCR primers were synthesized by Shanghai Sangon Biotechnology Co., Ltd. (Shanghai, China) (**Table 1**). The cDNA was subjected to real-time PCR reaction via using TaqMan® MicroRNA Assays and TaqMan® gene expression premix (ABI). U6 and glyceraldehyde-3-phosphate dehydrogenase (GAPDH) were the loading controls. The data were analyzed via $2^{-\Delta\Delta Ct}$ method.

Western blot analysis

The protein in myocardial tissues was extracted by Radio-Immunoprecipitation assay cell lysis buffer (Thermo Fisher Scientific, Rockford, IL,

Table 1. Primer sequences

	Primer sequences
MiR-378	Forward: 5'-CTGAGACTGGACTTGGAGTC-3'
	Reverse: 5'-GTGCAGGGTCCGAGGT-3'
U6	Forward: 5'-TGCGGGTGCTCGCTTCGGCAGC-3'
	Reverse: 5'-CCAGTGCAGGGTCCGAGGT-3'
Bcl-2	Forward: 5'-CTGTGCTGCTATCCTGC-3'
	Reverse: 5'-TGCAGCCACAATACTGT-3'
Bax	Forward: 5'-CCCGAGAGGTCTTTTTCCGAG-3'
	Reverse: 5'-CCAGCCCATGATGGTTCTGAT-3'
Caspase-3	Forward: 5'-CCATCCTTCAGTGGTGGACA-3'
	Reverse: 5'-TTGAGGCTGCTGCATAATCG-3'
MAPK1	Forward: 5'-TCTCCCGCACAAAAATAAGG-3'
	Reverse: 5'-GCCAGAGCCTGTTCAACTTC-3'
GAPDH	Forward: 5'-AAGAAGGTGGTGAAGCAGGC-3'
	Reverse: 5'-TCCACCACCCTGTTGCTGTA-3'

Note: MiR-378, MicroRNA-378; Bcl-2, B-cell lymphoma 2; Bax, Bcl-2-associated X; MAPK1, mitogen-activated protein kinase 1; GAPDH, glyceraldehyde-3-phosphate dehydrogenase.

USA), and the protein concentration was measured using a protein concentration assay kit (Sigma, St Louis, Missouri, USA). The protein was implemented with sodium dodecyl sulphate polyacrylamide gel electrophoresis, and transferred to the membrane via semi-dry method. Then the membrane was incubated with primary antibodies MAPK1 (1:500, Cell Signaling Technology, Beverly, MA, USA) and GAPDH (1:500) (Santa Cruz Biotechnology, Inc, Santa Cruz, CA, USA), the secondary antibody immunoglobulin G/horseradish peroxidase for 1 h, exposed and developed. GAPDH was used as the loading control. Image analysis software BandScan 5.0 was used for semi-quantitative analysis of relative protein expression.

Dual luciferase reporter gene assay

Jefferson online prediction software was used to predict the targeting relationship between miR-378 and MAPK1 and the binding sites of miR-378 and MAPK1-3' untranslated regions (UTR). PCR amplification of MAPK1 3'UTR fragments was implemented. The wild type (WT) and mutant type (MUT) recombinant plasmids were extracted by plasmid extraction kit (ThermoFisher), double enzyme-digested via restriction enzymes Xba I and Xho I, and the enzyme-digested products were purified and recycled again. T4DNA ligase was used to connect with fluorescein reporter carrier pmir-GLO, and DH5α competent E. coli was transformed, and extraction of plasmids, Xba I and Xho I double enzyme-digestion preliminary evaluation, sequencing were implemented. The WT and MUT recombinant double luciferase reporter plasmids were constructed, and named MAPK1-WT and MAPK1-MUT. The cultured 293T cells (American Type Culture Collection, VA, USA) were divided into 4 groups and co-transfected with miR-378 mimic/mimic NC and MAPK1-WT/MAPK1-MUT. The 293T cells were collected after transfection for 30 h, and the luciferase activities of firefly and renilla were detected by fluorescence detector with the dual luciferase reporter assay kit (Promega, Madison, WI, USA).

Statistical analysis

SPSS 21.0 (IBM Corp., Armonk, NY, USA) was used to analyze the data. The measurement data were expressed as mean ± standard deviation. The t test was used for two-group comparison in the data subjected to normal distribution. One-way analysis of variance (ANOVA) was used for comparison among multiple groups, and Tukey's post hoc test for pairwise comparison. *P* was a bilateral test, and predictors were kept if they were significant at a *P* value of 0.05 or smaller.

Results

Up-regulating miR-378 improves hemodynamics and myocardial injury in MI/RI mice

Hemodynamic, myocardial enzyme-, and oxidative stress-related indicators were detected. It was manifested that a decrease was seen in LVSP and ± dp/dt_{max} values, SOD, GSH-Px and CAT activities, and NO content, while an increase in LVEDP value, AST, CK, CK-MB and LDH activities, as well as MDA content in MI/RI mice. Up-regulating miR-378 would improve hemodynamics and myocardial injury, and impair oxidative stress in MI/RI mice while down-regulating miR-378 exerted oppositely. The effects induced by down-regulating miR-378 were reversed by suppression of MAPK1 (**Figure 1A-L**).

HE staining reflected that no obvious pathomorphological changes were observed in sham-operated mice. In MI/RI mice, inflammatory cell infiltration in the myocardial interstitium, and sarcomere fracture, disappearance and necro-

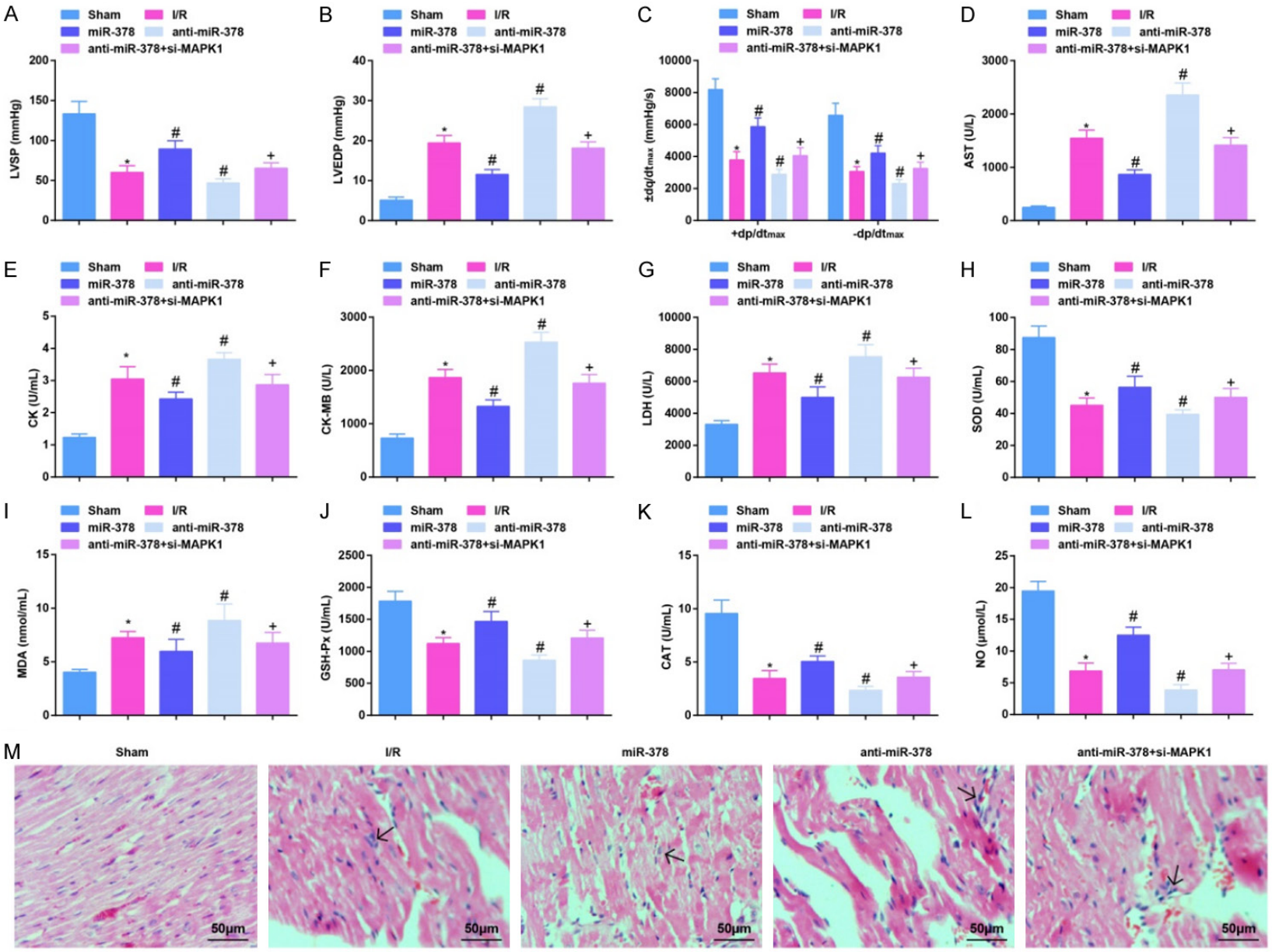
A
B
C
D
E
F
G
H
I
J
K
L
M
Sham
I/R
miR-378
anti-miR-378
anti-miR-378+si-MAPK1
LVSP (mmHg)
LVEDP (mmHg)
±dq/dtmax (mmHg/s)
+dp/dtmax
-dp/dtmax
AST (U/L)
CK (U/mL)
CK-MB (U/L)
LDH (U/L)
SOD (U/mL)
MDA (nmol/mL)
GSH-Px (U/mL)
CAT (U/mL)
NO (μmol/L)
50μm

Figure 1. Up-regulating miR-378 alleviates hemodynamics and myocardial injury in MI/RI mice. (A, B) The value of LVSP and LVEDP in MI/RI mice after up-regulating miR-378; (C) The value of ± dp/dt_{max} in MI/RI mice after up-regulating miR-378; (D-G) The activities of AST, CK, CK-MB and LDH in MI/RI mice after up-regulating miR-378; (H-L) The levels of SOD, MDA, GSH-Px, CAT and NO in MI/RI mice after up-regulating miR-378; (M) HE staining results in MI/RI mice after up-regulating miR-378 (× 200; Scale bar = 50 μm); * vs the sham group, $P < 0.05$; # vs the I/R group, $P < 0.05$; + vs the anti-miR-378 group, $P < 0.05$; 6 mice in each group (A-C) and 5 mice in each group (D-M). The data were expressed in the form of mean ± standard deviation. One-way ANOVA was used for data analysis, and Tukey's post hoc test was used for pairwise comparison after ANOVA analysis.

sis were observed. After up-regulating miR-378, myocardial injury was attenuated, necrosis and dissolution of cardiomyocytes were reduced and a small amount of inflammatory cells infiltration was manifested in mice with MI/RI. After down-regulating miR-378 in mice with MI/RI, severe myocardial injury and a large number of inflammatory cell infiltration were seen. In mice treated with anti-miR-378 and si-MAPK1, the situation was lighter than those treated anti-miR-378 only, but inflammatory cell infiltration and necrosis were still observed in the myocardial interstitial (**Figure 1M**). The results indicated that miR-378 improves hemodynamics and myocardial injury in MI/RI mice while silencing MAPK1 reversed the effects induced by down-regulation of miR-378.

Up-regulating miR-378 reduces apoptosis rate and inflammatory infiltration in MI/RI mice

TUNEL staining detecting cardiomyocyte apoptosis, RT-qPCR detecting apoptosis-associated factors, together with ELISA measuring inflammatory factors in serum reflected that the apoptosis rate of cardiomyocytes, Bax and Caspase-3 mRNA expression, and TNF-α, IL-6 and IL-1β contents were obviously increased, and Bcl-2 was clearly reduced in MI/RI mice. Restoring miR-378 suppressed cardiomyocyte apoptosis and inflammatory response in MI/RI mice. Reducing miR-378 in MI/RI mice promoted cardiomyocyte apoptosis and inflammatory response, which were reversed by down-regulation of MAPK1 (**Figure 2A-D**).

To further demonstrate the effect of miR-378 and MAPK1 on inflammatory infiltration in MI/RI mice, CD45 expression was detected by immunohistochemistry. Fewer CD45-expressed brown-yellow particles were observed on the cell membrane of the sham-operated mice. Much CD45-expressed brown-yellow particles were expressed in the inflammatory infiltration site in MI/RI mice, which could be suppressed by elevating miR-378. After down-regulation of miR-378, CD45-expressed brown-yellow particles increased, which would be reversed by down-regulation of MAPK1 (**Figure 2E**).

RT-qPCR and western blot analysis examining miR-378 and MAPK1 expression in myocardial tissues revealed that miR-378 level was reduced while MAPK1 was elevated in MI/RI mice. However, elevating miR-378 would raise miR-378 and inhibit MAPK1 levels while suppressing miR-378 had the opposite effects. Depleting MAPK1 reversed the impact of down-regulated miR-378 on MAPK1 expression in mice (**Figure 2F-H**).

It was suggestive that miR-378 attenuated cardiomyocyte apoptosis and inflammation in mice after MI/RI, and knockdown of MAPK1 reversed the effects induced by down-regulation of miR-378.

Restoring miR-378 further enhances ISO-induced improvement of hemodynamics and myocardial damage in MI/RI mice

When inspecting the effects of ISO on hemodynamics and myocardial damage in MI/RI mice, it was showed that ISO treatment increased LVSP, ± dp/dt_{max}, SOD, GSH-Px, CAT activity and NO content, as well as decreased LVEDP value, AST, CK, CK-MB, LDH activity and MDA content. Up-regulated miR-378 could enhance the effects of ISO treatment on MI/RI (**Figure 3A-L**).

HE staining showed that the myocardial injury in mice treated with ISO was attenuated, with necrosis and dissolution of cardiomyocytes and a small amount of inflammatory cells infiltration. The structure of myocardial tissues in mice treated with ISO and up-regulated miR-378 was close to that of normal myocardium (**Figure 3M**). It showed that up-regulated miR-378 further improved ISO-attenuated hemodynamics and myocardial injury in MI/RI mice.

Elevating miR-378 further strengthens the ISO-induced effects on apoptosis rate and inflammatory infiltration in MI/RI mice

Detected by various assays, it was indicated that ISO treatment reduced the apoptosis rate of cardiomyocytes, suppressed Bax and

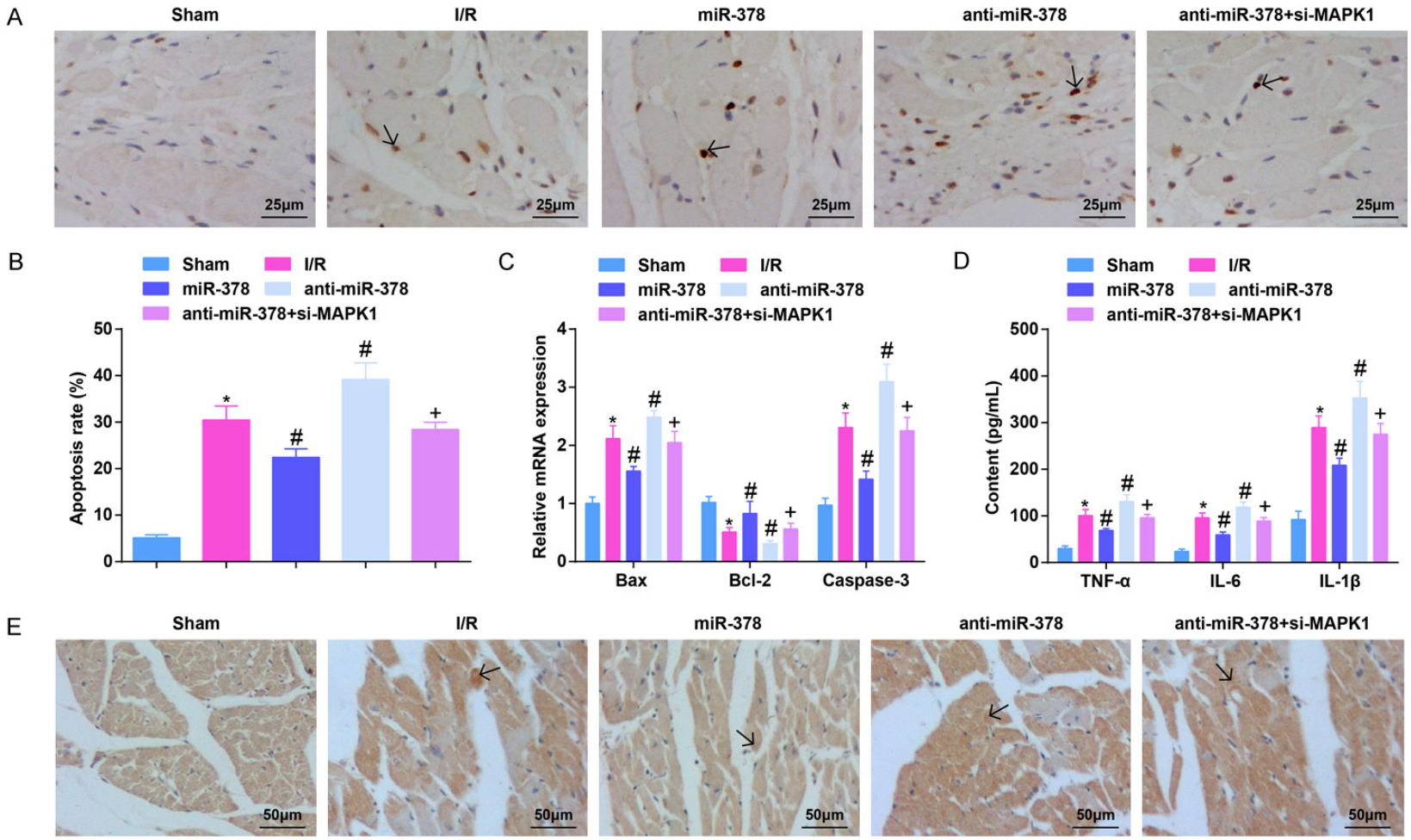
A
Sham
I/R
miR-378
anti-miR-378
anti-miR-378+si-MAPK1
25μm
B
Apoptosis rate (%)
C
Relative mRNA expression
Bax
Bcl-2
Caspase-3
D
Content (pg/mL)
TNF-α
IL-6
IL-1β
E
50μm

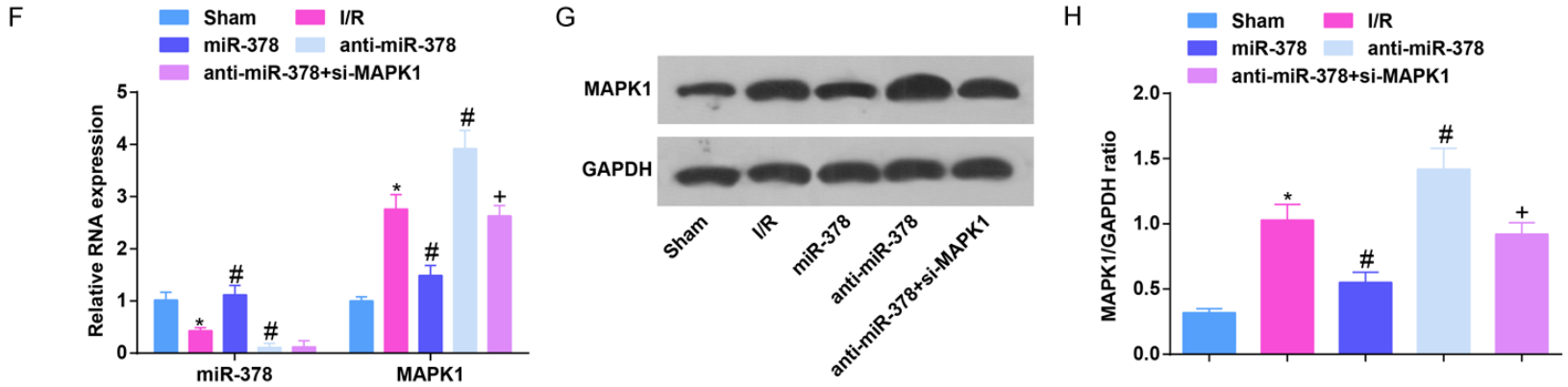

Figure 2. Up-regulating miR-378 decreases apoptosis rate and inflammatory infiltration in MI/RI mice. A. TUNEL staining results in MI/RI mice after up-regulating miR-378 (× 400; Scale bar = 25 μm); B. The apoptosis of cardiomyocytes in myocardial tissues detected via TUNEL staining; C. Bax, Bcl-2 and Caspase-3 mRNA expression in myocardial tissues in MI/RI mice after up-regulating miR-378 detected via RT-qPCR; D. The expression of TNF-α, IL-6, and IL-1β in serum in MI/RI mice after up-regulating miR-378 detected via ELISA; E. CD45 immunohistochemistry results in MI/RI mice after up-regulating miR-378 (× 200; Scale bar = 50 μm); F. The expression of miR-378 and MAPK1 in MI/RI mice after up-regulating miR-378 detected via RT-qPCR; G. Protein bands of MAPK1; H. The protein expression of MAPK1 in MI/RI mice after up-regulating miR-378; * vs the sham group, $P < 0.05$; # vs the I/R group, $P < 0.05$; + vs the anti-miR-378 group, $P < 0.05$; 5 mice in each group. The data were expressed in the form of mean ± standard deviation. One-way ANOVA was used for data analysis, and Tukey's post hoc test was used for pairwise comparison after ANOVA analysis.

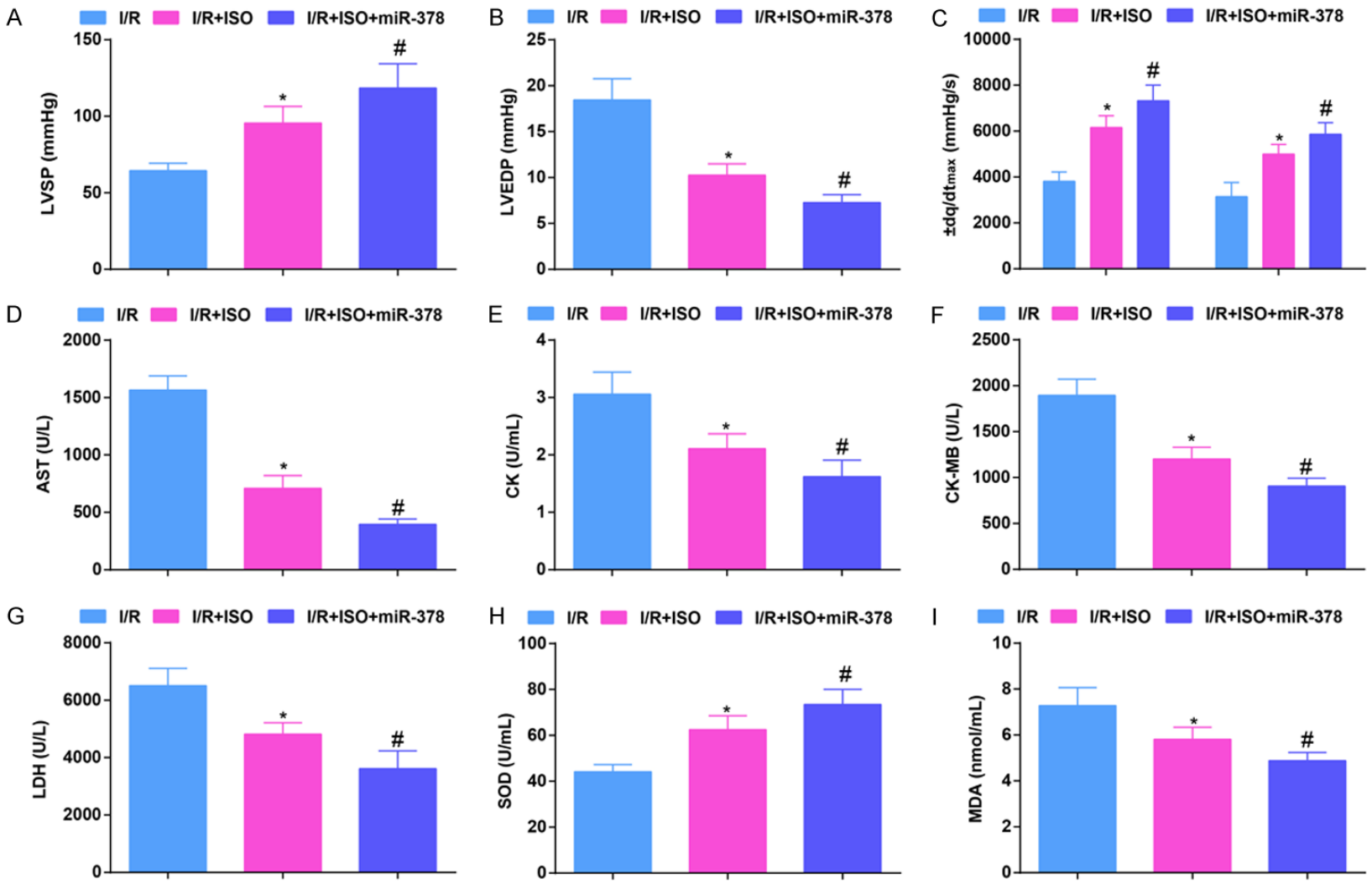
A
I/R
I/R+ISO
I/R+ISO+miR-378
LVSP (mmHg)
150
100
50
0
*
#
B
I/R
I/R+ISO
I/R+ISO+miR-378
LVEDP (mmHg)
25
20
15
10
5
0
*
#
C
I/R
I/R+ISO
I/R+ISO+miR-378
±dq/dtmax (mmHg/s)
10000
8000
6000
4000
2000
0
*
#
*
#
D
I/R
I/R+ISO
I/R+ISO+miR-378
AST (U/L)
2000
1500
1000
500
0
*
#
E
I/R
I/R+ISO
I/R+ISO+miR-378
CK (U/mL)
4
3
2
1
0
*
#
F
I/R
I/R+ISO
I/R+ISO+miR-378
CK-MB (U/L)
2500
2000
1500
1000
500
0
*
#
G
I/R
I/R+ISO
I/R+ISO+miR-378
LDH (U/L)
8000
6000
4000
2000
0
*
#
H
I/R
I/R+ISO
I/R+ISO+miR-378
SOD (U/mL)
100
80
60
40
20
0
*
#
I
I/R
I/R+ISO
I/R+ISO+miR-378
MDA (nmol/mL)
10
8
6
4
2
0
*
#

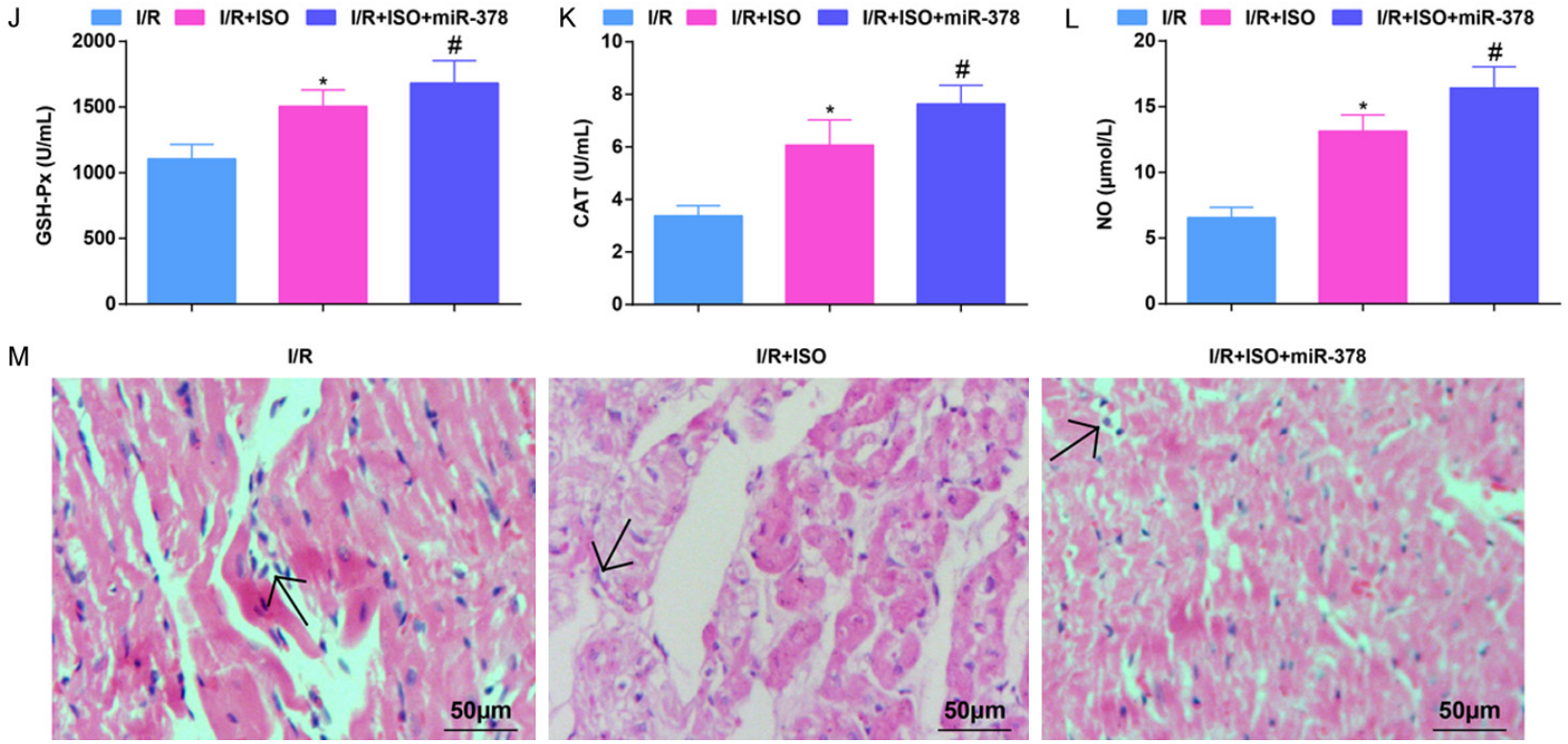

Figure 3. Restoring miR-378 further enhances the ISO-mediated improvement of hemodynamics and myocardial damage in MI/RI mice. (A, B) The values of LVSP and LVEDP in MI/RI mice after ISO treatment and up-regulating miR-378; (C) The values of ± dp/dt_{max} in MI/RI mice after ISO treatment and up-regulating miR-378; (D-G) The levels of AST, CK, CK-MB and LDH in MI/RI mice after ISO treatment and up-regulating miR-378; (H-L) The levels of oxidative stress-related indices SOD, MDA, GSH-Px, CAT and NO in MI/RI mice after ISO treatment and up-regulating miR-378; (M) HE staining results in MI/RI mice after ISO treatment and up-regulating miR-378 (× 200; Scale bar = 50 μm); * vs the I/R group, $P < 0.05$; # vs the I/R + ISO group, $P < 0.05$; 6 mice in each group (A-C) and 5 mice in each group (D-M). The data were expressed in the form of mean ± standard deviation. One-way ANOVA was used for data analysis, and Tukey's post hoc test was used for pairwise comparison after ANOVA analysis.

Caspase-3 mRNA expression, and TNF-α, IL-6 and IL-1β levels, and reduced CD45-expressed brown-yellow particles in MI/RI mice. Up-regulating miR-378 further reduced cardiomyocyte apoptosis and inflammation in MI/RI mice (**Figure 4A-E**).

miR-378 expression was found to elevate while MAPK1 expression to suppress in mouse myocardial tissues in response to ISO treatment. miR-378 up-regulation after ISO treatment further enhanced miR-378 and reduced MAPK1 levels (**Figure 4F-H**).

It was summarized that up-regulating miR-378 further enhanced the function of ISO in reducing apoptosis rate and inflammatory infiltration in MI/RI mice.

MAPK1 is the direct target gene of miR-378

Dual luciferase reporter gene assay was used to determine whether miR-378 regulated the activity of luciferase in the 3'UTR of MAPK1. The results showed that the luciferase activity of MAPK1 was distinctly decreased in 293T cells co-transfected with MAPK1-WT and miR-378 mimic, fully confirming that miR-378 directly regulated MAPK1 (**Figure 5A**, **5B**).

Discussion

MI/RI is a clinically vital problem connected with coronary artery bypass graft surgery [18]. A study has manifested that emulsified ISO is cardioprotective in MI/RI [19]. The mechanism of miR-378 has also been described in the cerebral ischemic injury [11]. In the meantime, MAPK signaling pathway has been demonstrated to participate in butorphanol protection on MI/RI rats [14]. Nevertheless, the literature about the association of miR-378 or MAPK1 with MI/RI is not presented. Hence, the destination of the study was to figure out the mechanism of ISO post-treatment on mice with MI/RI by modulating miR-378/MAPK1 axis.

The observations of the study were that reduced miR-378 and elevated MAPK1 existed in MI/RI. Accordingly, evidences have found that miR-378 level is markedly reduced in N2A cells after oxygen-glucose deprivation operation in cerebral ischemic injury and intestinal I/R injury [10, 11]. In addition, some studies have demonstrated that MAPK expression or its signaling pathway is clearly elevated in MI/RI [13, 14]. One interesting observation was that ISO elevated miR-378 to suppress MAPK1 level, and miR-378 targeted MAPK1. ISO has been recorded to elevate miRNA expression, such as miR-9 and miR-21 in embryonic stem cell self-renewal and neural differentiation of rats model [20, 21], but the regulatory mechanism of ISO for miR-378 is not researched. In fact, ISO can repress p38 MAPK activity during MI/RI and phosphorylated p38 MAPK in microglial cells [22, 23]. As to the targeting relation between miR-378 and MAPK1, studies have previously confirmed that miR-378 negatively regulates MAPK1 expression [24, 25].

The most obvious finding to emerge from the analysis was that ISO improved hemodynamics and myocardial injury and reduces apoptosis rate and inflammatory infiltration in MI/RI mice. It suits well with that ISO can, through repressing the p38 MAPK signaling pathway, decrease the oxidative stress response and relieve the pathological damage in cardiomyocytes from MI/RI [26]. In addition, a study has indicated that ISO preprocessing with captopril treatment eases MI/RI by attenuating oxidative stress and inflammation [7]. Moreover, ISO preconditioning has protective effects by reducing Caspase-3 expression and TNF-α production in a rabbit model of I/R injury [8, 27, 28]. This study also revealed that up-regulating miR-378 further enhanced the protective effects of ISO on MI/RI mice. It has been demonstrated that up-regulation of miR-378 lightens ischemia-induced apoptosis in cardiacmyocytes [29]. At the same time, silenced miR-378 may be used as a sensitive diagnostic or prognostic biomarker for acute myocardial infarction patients [30]. Also, mice genetically with absence of miR-378 and miR-378* manifest enhanced oxidative ability of insulin-target tissues in control of mitochondrial metabolism and systemic energy homeostasis [31].

Furthermore, our study suggested that ISO post-treatment may up-regulate miR-378 to improve MI/RI in mice, which may be related to down-regulation of MAPK1. A similar finding is also reported by Zhu *et al.* that MAPK1 turns around the repressive effects of miR-217 on apoptosis of cervical cancer cells [32]. An inhibitor of MAPK3/MAPK1 after carrageenan manifests a decrease in inflammation [33]. This finding is consistent with that of Shen *et al.* who have pronounced that oxidative stress induced

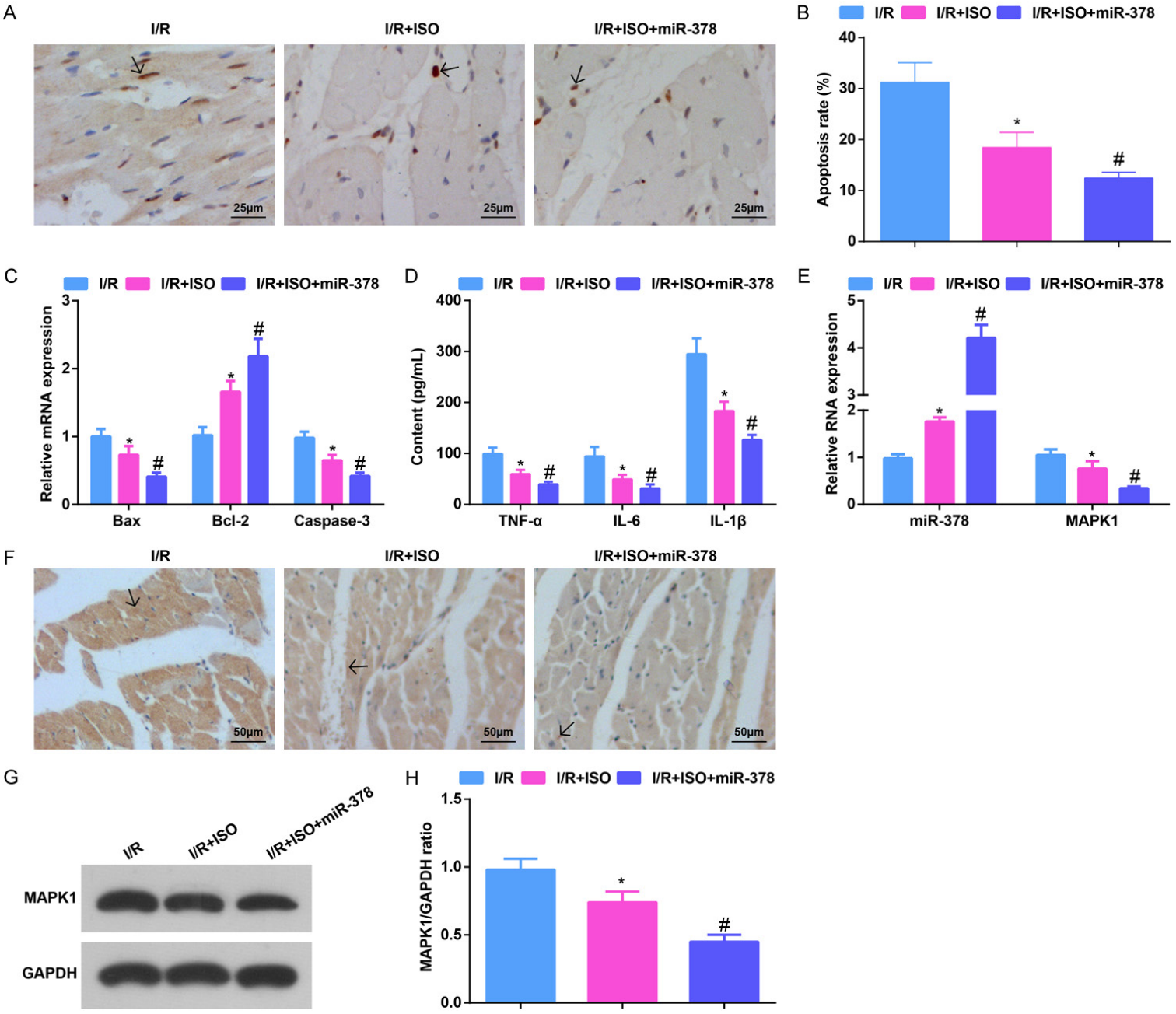
A
I/R
I/R+ISO
I/R+ISO+miR-378
25μm
B
Apoptosis rate (%)
C
Relative mRNA expression
Bax
Bcl-2
Caspase-3
D
Content (pg/mL)
TNF-α
IL-6
IL-1β
E
Relative RNA expression
miR-378
MAPK1
F
50μm
G
MAPK1
GAPDH
H
MAPK1/GAPDH ratio

Figure 4. Elevating miR-378 further strengthens the ISO-mediated effects on apoptosis rate and inflammatory infiltration in MI/RI mice. A. TUNEL staining results in MI/RI mice after ISO treatment and up-regulating miR-378 (× 400; Scale bar = 25 μm); B. The apoptosis of cardiomyocytes in myocardial tissues detected via TUNEL staining; C. Bax, Bcl-2 and Caspase-3 mRNA expression in myocardial tissues in MI/RI mice after ISO treatment and up-regulating miR-378 detected via RT-qPCR; D. The expression of TNF-α, IL-6, and IL-1β in serum in MI/RI mice after ISO treatment and up-regulating miR-378 detected via ELISA; E. The expression of miR-378 and MAPK1 in MI/RI mice after ISO treatment and up-regulating miR-378 detected via RT-qPCR; F. CD45 immunohistochemistry results in MI/RI mice after ISO treatment and up-regulating miR-378 (× 200; Scale bar = 50 μm); G. Protein bands of MAPK1; H. The protein expression of MAPK1 in MI/RI mice after ISO treatment and up-regulating miR-378; * vs the I/R group, $P < 0.05$; # vs the I/R + ISO group, $P < 0.05$; 5 mice in each group. The data were expressed in the form of mean ± standard deviation. One-way ANOVA was used for data analysis, and Tukey's post hoc test was used for pairwise comparison after ANOVA analysis.

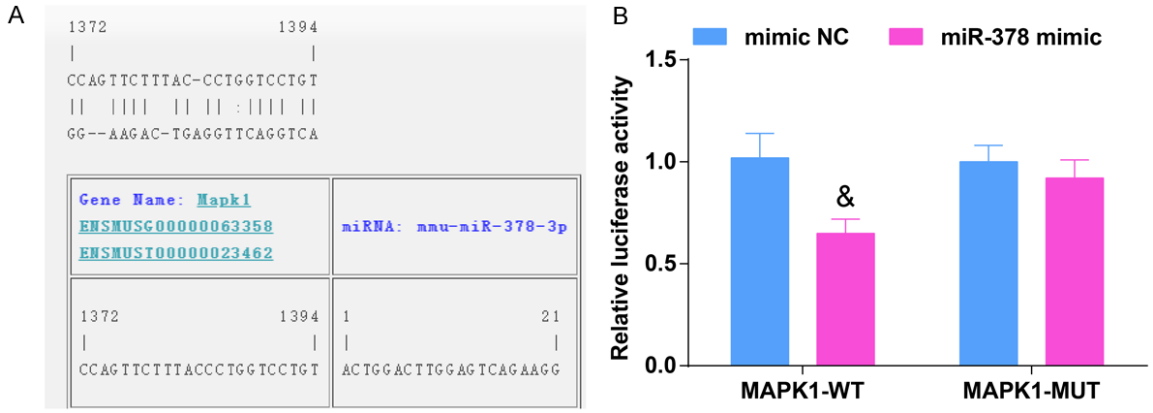

Figure 5. MAPK1 is the direct target gene of miR-378. A. The binding sites of MAPK1 and miR-378, N = 3; B. Luciferase assay verified the targeting relationship between MAPK1 and miR-378, N = 3. & vs the mimic NC group, $P < 0.05$. The data were expressed in the form of mean ± standard deviation, and the t test was used for two-group comparison.

growth inhibitor 1 is related to MAPK1/3 in mouse spermatogenesis [34].

All in all, this study highlights that ISO post-treatment may improve MI/RI in mice through up-regulation of miR-378 and down-regulation of MAPK1, and provides a potential treatment for MI/RI. The findings provide a new insight into the mechanism of MI/RI. Future studies on the current topic are still recommended.

Acknowledgements

We would like to acknowledge the reviewers for their helpful comments on this paper. This work was supported by the Research on Basic and Advanced Technology of Henan Province (2014) (No. 142300410087, perioperative application of etomidate in children with congenital heart disease); the Henan Medical Science and Technology Research Plan (2018, Joint Construction Project) (No. 2018020692, research on the effect of naborphine on the recovery of children with severe caries under general anesthesia) and the Science and Technology Development Plan of Zhengzhou (2015) (No. 20150172, application of dexmedetomidine in anesthesia for operation of digestive tract malformation of newborn; No. 20150171, a comparative study of different doses of dexmedetomidine in prevention of cough and restlessness during recovery and extubation of bronchial foreign bodies in children; No. 20150167, application of fast channel anesthesia in fast rehabilitation of children with transesophageal ultrasound-guided transcatheter closure).

Disclosure of conflict of interest

None.

Address correspondence to: Dr. Yanmei Yang, Anesthesiology Department, Kaifeng District of No.988 Hospital, PLA's Logistic Support Department, No. 3 Qian Street, Yuwangtai District, Kaifeng 475003, Henan, China. Tel: +86-0371-22258580; E-mail: yangyanmei269@163.com

References

[1] Sun T, Cheng YT, Yan LX, Krittanawong C, Qian W and Zhang HJ. LncRNA MALAT1 knockdown alleviates myocardial apoptosis in rats with myocardial ischemia-reperfusion through activating PI3K/AKT signaling pathway. Eur Rev Med Pharmacol Sci 2019; 23: 10523-10531.

[2] Bai Y, Li Z, Liu W, Gao D, Liu M and Zhang P. Biochanin A attenuates myocardial ischemia/reperfusion injury through the TLR4/NF-kappaB/NLRP3 signaling pathway. Acta Cir Bras 2019; 34: e201901104.

[3] Shen D, Chen R, Zhang L, Rao Z, Ruan Y, Li L, Chu M and Zhang Y. Sulodexide attenuates endoplasmic reticulum stress induced by myocardial ischaemia/reperfusion by activating the PI3K/Akt pathway. J Cell Mol Med 2019; 23: 5063-5075.

[4] Charles EJ, Tian Y, Zhang A, Wu D, Mehaffey JH, Gigliotti JC, Klibanov AL, Kron IL and Yang Z. Pulsed ultrasound attenuates the hyperglycemic exacerbation of myocardial ischemia-reperfusion injury. J Thorac Cardiovasc Surg 2021; 161: e297-e306.

[5] Chen Q, Liu Y, Ding X, Li Q, Qiu F, Wang M, Shen Z, Zheng H and Fu G. Bone marrow mesenchymal stem cell-secreted exosomes carrying microRNA-125b protect against myocardial ischemia reperfusion injury via targeting SIRT7. Mol Cell Biochem 2019; 465: 103-114.

[6] Joys S, Samra T, Kumar V, Mohanty M, Sodhi HBS, Mahajan S and Bhagat H. Comparison of postoperative delirium in patients anesthetized with isoflurane versus desflurane during spinal surgery: a prospective randomized controlled trial. Surg Neurol Int 2019; 10: 226.

[7] Tian Y, Li H, Liu P, Xu JM, Irwin MG, Xia Z and Tian G. Captopril pretreatment produces an additive cardioprotection to isoflurane preconditioning in attenuating myocardial ischemia reperfusion injury in rabbits and in humans. Mediators Inflamm 2015; 2015: 819232.

[8] Ran K, Zou DQ, Xiao YY, Chang YT, Duan KM, Ou YW and Li ZJ. Effects of isoflurane preconditioning in the delayed phase on myocardial tumor necrosis factor alpha levels and caspase-3 protein expression in a rabbit model of ischemia-reperfusion injury. Genet Mol Res 2015; 14: 7267-7273.

[9] Ding N, Luo M, Liao XL, Bao QY, Li RY and Wu B. MicroRNA-378 promotes the malignant progression of oral squamous cell carcinoma by mediating FOXN3. Eur Rev Med Pharmacol Sci 2019; 23: 6202-6210.

[10] Li Y, Wen S, Yao X, Liu W, Shen J, Deng W, Tang J, Li C and Liu K. MicroRNA-378 protects against intestinal ischemia/reperfusion injury via a mechanism involving the inhibition of intestinal mucosal cell apoptosis. Cell Death Dis 2017; 8: e3127.

[11] Zhang N, Zhong J, Han S, Li Y, Yin Y and Li J. MicroRNA-378 alleviates cerebral ischemic injury by negatively regulating apoptosis executioner Caspase-3. Int J Mol Sci 2016; 17: 1427.

[12] Xu M, Zhou K, Wu Y, Wang L and Lu S. Linc00161 regulated the drug resistance of ovarian cancer by sponging microRNA-128 and modulating MAPK1. Mol Carcinog 2019; 58: 577-587.

[13] Xu T, Zhang K, Kan F, Li F, Yu B, Du W and Nie H. Adeno-associated Virus 9-mediated small RNA interference of TLR4 alleviates myocardial ischemia and reperfusion injury by inhibition of the NF-kappaB and MAPK signaling pathways in rats. Curr Mol Med 2019; 19: 127-135.

[14] Wang H, Wang JL, Ren HW, He WF and Sun M. Butorphanol protects on myocardial ischemia/reperfusion injury in rats through MAPK signaling pathway. Eur Rev Med Pharmacol Sci 2019; 23: 10541-10548.

[15] Minutoli L, Antonuccio P, Polito F, Bitto A, Squadrito F, Di Stefano V, Nicotina PA, Fazzari C, Maisano D, Romeo C and Altavilla D. Mitogen-activated protein kinase 3/mitogen-activated protein kinase 1 activates apoptosis during testicular ischemia-reperfusion injury in a nuclear factor-kappaB-independent manner. Eur J Pharmacol 2009; 604: 27-35.

[16] Tan H, Qi J, Fan BY, Zhang J, Su FF and Wang HT. MicroRNA-24-3p attenuates myocardial ischemia/reperfusion injury by suppressing RIPK1 expression in mice. Cell Physiol Biochem 2018; 51: 46-62.

[17] Qiao S, Olson JM, Paterson M, Yan Y, Zaja I, Liu Y, Riess ML, Kersten JR, Liang M, Warltier DC, Bosnjak ZJ and Ge ZD. MicroRNA-21 mediates isoflurane-induced Cardioprotection against ischemia-reperfusion injury via Akt/nitric oxide synthase/mitochondrial permeability transition pore pathway. Anesthesiology 2015; 123: 786-798.

[18] Dwaich KH, Al-Amran FG, Al-Sheibani BI and Al-Aubaidy HA. Melatonin effects on myocardial ischemia-reperfusion injury: Impact on the outcome in patients undergoing coronary artery bypass grafting surgery. Int J Cardiol 2016; 221: 977-986.

[19] Rao Y, Wang YL, Chen YQ, Zhang WS and Liu J. Protective effects of emulsified isoflurane after myocardial ischemia-reperfusion injury and its mechanism in rabbits. Chin J Traumatol 2009; 12: 18-21.

[20] Zhang L, Zhang Y, Hu R, Yan J, Huang Y, Jiang J, Yang Y, Chen Z and Jiang H. Isoflurane inhibits embryonic stem cell self-renewal and neural differentiation through miR-9/E-cadherin signaling. Stem Cells Dev 2015; 24: 1912-1922.

[21] Olson JM, Yan Y, Bai X, Ge ZD, Liang M, Kriegel AJ, Twaroski DM and Bosnjak ZJ. Up-regulation of microRNA-21 mediates isoflurane-induced protection of cardiomyocytes. Anesthesiology 2015; 122: 795-805.
[22] Ran K, Duan KM, Zou DQ, Li ZJ, Jin LY and Chang YT. Effect of isoflurane delayed preconditioning on myocardial ischemia reperfusion injury in rabbits. Zhong Nan Da Xue Xue Bao Yi Xue Ban 2008; 33: 146-150.
[23] Ryu JH, Wang Z, Fan D, Han SH, Do SH and Zuo Z. Isoflurane attenuates mouse microglial engulfment induced by lipopolysaccharide and interferon-gamma possibly by inhibition of p38 mitogen-activated protein kinase. Neuroreport 2016; 27: 1101-1105.
[24] Diao L, Wang S and Sun Z. Long noncoding RNA GAPLINC promotes gastric cancer cell proliferation by acting as a molecular sponge of miR-378 to modulate MAPK1 expression. Onco Targets Ther 2018; 11: 2797-2804.
[25] Chen QG, Zhou W, Han T, Du SQ, Li ZH, Zhang Z, Shan GY and Kong CZ. MiR-378 suppresses prostate cancer cell growth through downregulation of MAPK1 in vitro and in vivo. Tumour Biol 2016; 37: 2095-2103.
[26] Zhou Y, Peng DD, Chong H, Zheng SQ, Zhu F and Wang G. Effect of isoflurane on myocardial ischemia-reperfusion injury through the p38 MAPK signaling pathway. Eur Rev Med Pharmacol Sci 2019; 23: 1342-1349.
[27] Wang W, Zhu M, Xu Z, Li W, Dong X, Chen Y, Lin B and Li M. Ropivacaine promotes apoptosis of hepatocellular carcinoma cells through damaging mitochondria and activating caspase-3 activity. Biol Res 2019; 52: 36.
[28] Zhang J, Chi H, Xiao H, Tian X, Wang Y, Yun X and Xu Y. Interleukin 6 (IL-6) and tumor necrosis factor alpha (TNF-alpha) single nucleotide polymorphisms (snps), inflammation and metabolism in gestational diabetes mellitus in Inner Mongolia. Med Sci Monit 2017; 23: 4149-4157.
[29] Fang J, Song XW, Tian J, Chen HY, Li DF, Wang JF, Ren AJ, Yuan WJ and Lin L. Overexpression of microRNA-378 attenuates ischemia-induced apoptosis by inhibiting caspase-3 expression in cardiac myocytes. Apoptosis 2012; 17: 410-423.
[30] Ali, Sheikh S, Xia K, Li F, et al. GW27-e0556 Clinical impact of circulating miR-208b, miR-499 and miR-378 in acute myocardial infarction. J Am Coll Cardiol 2016; 68: C94.
[31] Carrer M, Liu N, Grueter CE, Williams AH, Frisard MI, Hulver MW, Bassel-Duby R and Olson EN. Control of mitochondrial metabolism and systemic energy homeostasis by microRNAs 378 and 378*. Proc Natl Acad Sci U S A 2012; 109: 15330-15335.
[32] Zhu L, Yang S and Wang J. miR-217 inhibits the migration and invasion of HeLa cells through modulating MAPK1. Int J Mol Med 2019; 44: 1824-1832.
[33] Di Paola R, Crisafulli C, Mazzon E, Genovese T, Paterniti I, Bramanti P and Cuzzocrea S. Effect of PD98059, a selective MAPK3/MAPK1 inhibitor, on acute lung injury in mice. Int J Immunopathol Pharmacol 2009; 22: 937-950.
[34] Shen X, Niu C, Guo J, Xia M, Xia J, Hu Y and Zheng Y. Stra8 may inhibit apoptosis during mouse spermatogenesis via the AKT signaling pathway. Int J Mol Med 2018; 42: 2819-2830.